Biochimica et Biophysica Acta 1843 (2014) 640–651

Contents lists available at ScienceDirect

Biochimica et Biophysica Acta

journal homepage: www.elsevier.com/locate/bbamcr

Poly(ADP-ribose) polymerase-1 and its cleavage products differentially modulate cellular protection through NF-kB-dependent signaling

Paola Castri [a,*], Yang-ja Lee [a], Todd Ponzio [b], Dragan Maric [c], Maria Spatz [a], Joliet Bembry [a], John Hallenbeck [a]

[a] Stroke Branch, National Institutes of Neurological Disorders and Stroke (NINDS), National Institutes of Health (NIH), Bethesda, MD, USA
[b] Laboratory of Neurochemistry, NINDS, NIH, Bethesda, USA
[c] Flow Cytometry Core Facility, NINDS, NIH, Bethesda, USA

ARTICLE INFO

Article history:
Received 18 March 2013
Received in revised form 20 November 2013
Accepted 5 December 2013
Available online 12 December 2013

Keywords:
PARP-1
ARTD1
Brain ischemia
OGD
NF-kB

ABSTRACT

Poly(ADP-ribose) polymerase-1 (PARP-1) and its cleavage products regulate cell viability and NF-kB activity when expressed in neurons. PARP-1 cleavage generates a 24 kDa (PARP-1_{24}) and an 89 kDa fragment (PARP-1_{89}). Compared to WT (PARP-1_{WT}), the expression of an uncleavable PARP-1 (PARP-1_{UNCL}) or of PARP-1_{24} conferred protection from oxygen/glucose deprivation (OGD) or OGD/restoration of oxygen and glucose (ROG) damage in vitro, whereas expression of PARP-1_{89} was cytotoxic. Viability experiments were performed in SH-SY5Y, a human neuroblastoma cell line, as well as in rat primary cortical neurons. Following OGD, the higher viability in the presence of PARP-1_{UNCL} or PARP-1_{24} was not accompanied with decreased formation of poly(ADP-riboses) or higher NAD levels. PARP-1 is a known cofactor for NF-kB, hence we investigated whether PARP-1 cleavage influences the inflammatory response. All PARP-1 constructs mimicked PARP-1_{WT} in regard to induction of NF-kB translocation into the nucleus and its increased activation during ischemic challenge. However, expression of PARP-1_{89} construct induced significantly higher NF-kB activity than PARP-1_{WT}; and the same was true for NF-kB-dependent iNOS promoter binding activity. At a protein level, PARP-1_{UNCL} and PARP-1_{24} decreased iNOS (and lower levels of iNOS transcript) and COX-2, and increased Bcl-xL. The increased levels of NF-kB and iNOS transcriptional activities, seen with cytotoxic PARP-1_{89}, were accompanied by higher protein expression of COX-2 and iNOS (and higher levels of *INOS* transcript) and lower protein expression of Bcl-xL. Taken together, these findings suggest that PARP-1 cleavage products may regulate cellular viability and inflammatory responses in opposing ways during in vitro models of "ischemia".

Published by Elsevier B.V.

1. Introduction

Poly(ADP-ribose) polymerase 1 (PARP-1), also known as ARTD1 (diphtheria toxin-like-ADP-ribosyltransferase) [1,2], plays a role in the inflammatory pathogenesis of many central nervous system disorders including stroke [3–6]. A change in PARP-1 activity has been reported in ischemia–reperfusion damage involving complex mechanisms that are not completely understood, including regulation of DNA repair, cell death, transcription and inflammation [7].

Here we investigate a possible involvement of PARP-1, particularly its cleavage products, in the regulation of cell viability using in vitro models of ischemia (known as oxygen/glucose deprivation, OGD) or OGD/restoration of oxygen and glucose (ROG).

PARP-1 is known to have many functions and among them, two are well known, namely the detection and repair of DNA single strand breaks through poly(ADP-ribosyl)ation (PARylation) [8,9], and the regulation of transcription by coupling with many transcription factors such as NF-kB [10,11]. PARylation requires PARP-1 C-terminal domain catalytic activity, consuming NAD, and can influence NF-kB activity through direct addition of poly(ADP-riboses) (PARs) on to NF-kB itself [12,13]. PARP-1/ARTD1 contains an N-terminal DNA-binding domain (DBD), an automodification region, and a C-terminal catalytic domain [14]. The caspase cleavage site $DEVD_{214}$ is situated in the DBD within the nuclear localization signal (NLS) [15]. PARP-1 is known to be cleaved at the $DEVD_{214}$ site by activated caspases 3 and 7 [16] leading to the formation of a 24 kDa and an 89 kDa fragment (Fig. 1A). Although the consequences of PARP-1 cleavage as well as of the effects of its two cleavage products remain unclear, depending on the intensity and type of stimuli that induce the cleavage itself, two main results have been reported, namely (1) the reduction of PARylation during DNA repair processes and (2) the modification of transcription activity of a PARP-1 bound protein complex that includes NF-kB. Generally, following massive DNA damage, the appearance of 24 kDa and 89 kDa PARP-1 fragments is widely accepted as a hallmark of apoptosis [16]. However, the suggestion that PARP-1 cleavage would reduce PARylation and save the cells

Abbreviations: PARP-1, poly(ADP-ribose) polymerase 1; PARylation, poly(ADP-ribosyl)ation; NB, neuroblastoma; OGD, oxygen and glucose deprivation; 24 kDa PARP-1, 24 kDa fragment of PARP-1; 89 kDa PARP-1, 89 kDa fragment of PARP-1; NF-kB, nuclear factor-kappa B; tet, tetracycline

* Corresponding author at: Building 10, Room 5B06, Stroke Branch, National Institutes of Neurological Disorders and Stroke (NINDS), National Institutes of Health (NIH), 9000 Rockville Pike, Bethesda 20892, MD, USA. Tel.: +1 301 594 2514; fax: +1 301 402 2336.
E-mail address: castrip@mail.nih.gov (P. Castri).

0167-4889/$ – see front matter. Published by Elsevier B.V.
http://dx.doi.org/10.1016/j.bbamcr.2013.12.005

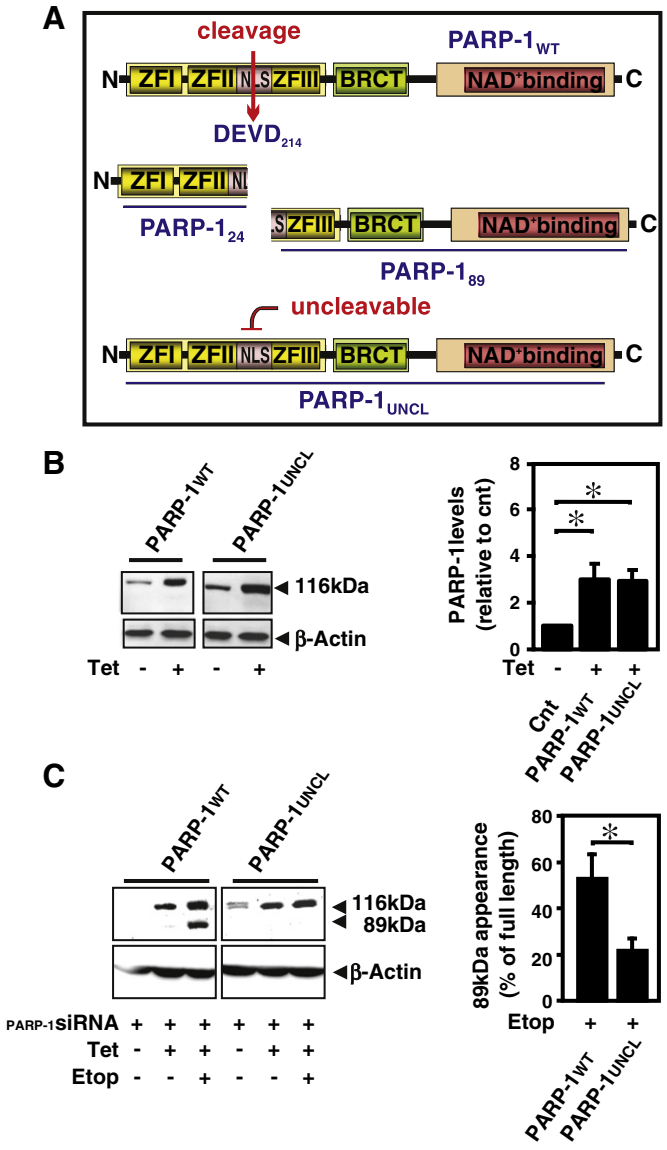

Fig. 1. Characterization of caspase-resistant PARP-1_{UNCL}. (A) PARP-1_{WT} (top) is cleaved by activated caspases at the $DEVD_{214}$ site. Upon cleavage the two fragments, 24 and 89 kDa, are produced (middle). PARP-1_{UNCL} cannot be cleaved (bottom). DNA binding domain (DBD), automodification region containing the BRCT, and the catalytic domain are highlighted in yellow, green and pink, respectively. ZF = Zinc Finger domains I, II and III, NLS = Nuclear Localization Sequence, BRCT = Breast Cancer Suppressor Protein. (B) Western blots of total cell extracts showing tet-dependent over expression of PARP-1_{WT} or PARP-1_{UNCL} (left) and its quantification by densitometry (right), n = 9. (C) Western blots showing $DEVN_{214}$ resistance to caspase-induced cleavage (left) and corresponding density (right). n = 3. Etop = Etoposide. For B and C, data are expressed as mean ± SD,*$p < 0.02$.

from excessive energy (NAD^+, ATP) depletion still remains [17,18]. An alternative role for PARP-1 cleavage acting as a regulator of NF-kB transactivation is being increasingly investigated [10,19–23].

NF-kB is a central cellular module that regulates, among other things, the inflammatory response [24]. The major subtype of NF-kB consists of a hetero-dimer of subunits p50 and p65, which is kept inactive by the inhibitor of NF-kB protein (IKB) in the cytoplasm. Upon stimulation, IKB is ubiquitinated and degraded allowing NF-kB translocation to the nucleus where it binds to DNA and activates transcription. It has been shown in animal models that ischemia activates NF-kB leading to the inflammatory response, and that its inactivation is generally neuroprotective [25,26]. Reports also indicate that the activation of certain NF-kB-dependent pro and anti-inflammatory/protective genes is regulated by complex mechanisms that are still poorly understood [27].

Previous observations suggest that PARP-1 and NF-kB functions are interconnected in ischemic conditions [28–31]. One more layer of complexity is that not only is PARP-1 a cofactor for NF-kB, but the cleavage of PARP-1 further influences NF-kB activity. A few reports have suggested that PARP-1 cleavage may participate in transactivation of NF-kB in a pro-inflammatory fashion [11,23,32–34]. It is of particular interest that an uncleavable form of PARP-1 (PARP-1_{UNCL}) (Fig. 1A) in transgenic mice conferred protection from endotoxic shock, and intestinal and renal ischemia/reperfusion damage [23].

Therefore, the aim of this study was to shed light on the functional role of PARP-1 cleavage at the DEVD site and to investigate the role of each fragment produced in cell viability and the NF-kB transcriptional response during ischemic stress. Human neuroblastoma cells (SH-SY5Y) were used in models of "ischemia" (oxygen/glucose deprivation —OGD) to study four variants of PARP-1 (control PARP-1_{WT} and three experimental variants of PARP-1, PARP-1_{UNCL}, PARP-1_{24} and PARP-1_{89}) on (1) cell survival and (2) the transcriptional regulation of NF-kB-dependent proteins. Cell survival studies were extended in a complimentary model (OGD/ROG) using primary rat cortical neurons.

We found that the uncleavable PARP-1_{UNCL} as well as PARP-1_{24} were cytoprotective, and PARP-1_{89} was toxic. This study also suggests that PARP-1 cleavage or its fragments do not modify cellular levels of PARs or NAD levels, at least in our OGD model. However, NF-kB activity and the expression of certain downstream effectors were modulated by the different forms of PARP-1. These findings suggest that PARP-1 cleavage may play a role in the regulation of cell viability and NF-kB in response to OGD or OGD/ROG.

2. Materials and methods

2.1. Cell culture and transfection: SH-SY5Y and primary rat cortical neurons

Human neuroblastoma cells, SH-SY5Y (American Type Culture Collection, Manassas, VA, USA; Cat# CRL-2266), were cultured in Dulbecco's modified Eagle's medium (DMEM) supplemented with 10% heat-inactivated fetal bovine serum, 100 U/ml penicillin, and 100 mg/ml streptomycin (DMEM complete) in 5% CO_2 at 37 °C. Tetracycline (tet)-inducible stable transfectants were generated as previously described [35]. In particular, the constructs used were PARP-1_{WT}, PARP-1 $_{UNCL}$, PARP-1_{24} and PARP-1_{89}. See Section 2.2 "Cloning" for more details.

Lipofectamine RNAi max (Invitrogen) was used to transfect the cells with siRNA-PARP-1 (Target Sequence: 5′-ACGGTGATCGGTAGCAAC AAA-3′, FlexiTube, Qiagen) at a concentration of 25 nM. In experiments with siRNA, tet (1 μg/ml) was added at the same time as the siRNA in order to minimize the period of PARP-1 deprivation. All the experiments were performed using siRNA-PARP-1 with the exception of viability experiments for cells overexpressing PARP-1_{24} and PARP-1_{89}. siRNA-PARP-1 was not used for viability experiments conducted on primary cortical neurons from rats (where an effect was seen without the need of reducing the background from endogenous PARP-1). Control experiments were conducted using scramble siRNA (AllStars Negative Control siRNA, Qiagen) as negative control.

Primary cortical neurons were isolated from Sprague–Dawley rats at 2 days of age (P2) and cultured in Neurobasal Medium-A (NB-A) supplemented with B27, as previously reported [35] and plated at a density of 3.75×10^5 cells/ml. Experiments using cells isolated from rat brains were conducted in accordance with the Institutional Animal Care and Use Committee at the National Institute of Health guidelines.

Constructs for PARP-1_{WT}, PARP-1_{UNCL} and PARP-1_{24} were cloned into a custom made viral vector for Adeno-Associated Viruses (AAVs). See Section 2.2 "Cloning" for more details. Cortical neurons were transduced 3 days after isolation. At day 4 the medium was replaced and at day 6, after measuring the transfection efficiency, the cells were subjected to OGD for 6 h followed by ROG (15 h).

2.2. Cloning

Wild type PARP-1 plasmid was purchased from the Harvard Institute of Proteomics (plasmid ID HsCD00040600 http://plasmid.med.harvard.edu/PLASMID/Home.jsp) and the sequence was confirmed.

2.2.1. Cloning PARP-1_{WT}, PARP-1_{UNCL}, PARP-1_{24} and PARP-1_{89} into pcDNA4/TO vector

Constructs for wild type PARP-1_{WT}, PARP-1_{24} and PARP-1_{89} were amplified with appropriate restriction sites by PCR using the PARP-1_{WT} plasmid as a template. The primer sets used were as follows:

AflII(F)-5′-AGCTCTTAAGATGGCGGAGTCTTCGGAT-3′ and XhoI(R)-5′-ATCACTCGAGTTACCACAGGGAGGTCTT-3′ for PARP-1_{WT}; AflII(F)-5′-AGCTCTTAAGATGGATGGAGTGGATGAAG-3′ and XhoI(R)- 5′-ATCACTCGAGTTACCACAGGGAGGTCTT-3′ for PARP-1_{89}; EcoRI(F)-5′-AGCTGAATTCATGGCGGAGTCTTCGGAT-3′ and XbaI(R)-5′-CATCTAGATTATCCATCCACCTCATCGC-3′ for PARP-1_{24}.

Each PCR amplified DNA was cloned into pcDNA4/TO vector.

PARP-1 siRNA resistant mutants WT and PARP-1_{UNCL} $DEVN_{214}$ (GAT → AAT) were generated by using the QuickChange II or Quick Change Multi Site-directed Mutagenesis Kits (Stratagene, La Jolla, CA; Cat# 200523) as previously described [23]. Primers for siRNA resistant WT and PARP-1_{UNCL} were as follows: PARP-1_{UNCL} (F)-5′-GAAAAGGCGATGAGGTGAATG-3′ and PARP-1_{UNCL} (R)-5′-CACTTCATCCACTCCATTCACCTCATCGCCTTTTC-3′.

2.2.2. Cloning PARP-1_{WT}, PARP-1_{UNCL} and PARP-1_{24} into a viral vector suitable for packaging an Adeno-Associated Virus (AAV)

PARP-1_{WT}, PARP-1_{UNCL} and PARP-1_{24} were cloned into a viral vector using appropriate restriction sites, after amplification by PCR. Primers used for PARP-1_{WT} and PARP-1_{UNCL} were MefI(F)-5′-GTACCAATTGATGGCGGAGTCTTCGGATAAG-3′ and SalI(R)-5′-CGACGTGTCGACTTACCACAGGGAGGTCTTAA-3′. Primers used for PARP-1_{24} were EcoRI(F)-5′-AGCTGAATTCATGGCGGAGTCTTCGGAT-3′ and SalI(R)-5′-GTACCCGCGGTCCATCCACCTCATCGCCTTTTC-3′.

Each PCR amplified DNA was cloned into the pFBGR plasmid (a pFastBac™ variant obtained from Dr. Robert Kotin, NIH/NHLBI), a plasmid containing two AAV inverted terminal repeats (ITRs) flanking the CMV promoter and EGFP reporter. The EGFP is separated (not fused) from PARP-1 gene by a T2A region that allows measurement of transfection efficiency in addition to the overexpression of the gene of interest. Finally, the poly(A) tail was replaced with Woodchuck Hepatitis Virus Posttranscriptional Regulatory Element (WPRE) to enhance transcription. DH10Bac cells (Invitrogen) were transformed with donor AAV plasmids (WT, PARP-1_{UNCL}, or PARP-1_{24}) and plated on appropriate selection media [36]. Briefly, PARP-1 constructs containing baculovirus were added along with a second AAV-6 packaging baculovirus (generous gift from R. Kotin, NIH) which was chosen because we had found it to be the most efficient in transducing primary cortical neurons in our preliminary experiments among AAV-2, AAV-4, AAV-5, AAV-6, and AAV-8. Titering procedure of the final AAV was done according to previously described methods [36].

2.3. Oxygen and glucose deprivation (OGD), OGD/restoration of oxygen and glucose (ROG) and cell death assessment

OGD for SH-SY5Y or cortical neurons was performed as described previously [35]. The lengths of OGD were 15 h for SH-SY5Y cells and 6 h for cortical neurons, due to their increased sensitivity to the exposure. SH-SY5Y cells were assayed immediately after OGD to evaluate cell viability. In the cortical neurons, the OGD medium (PBS with 2 mM $MgCl_2$ and 1 mM $CaCl_2$) was replaced at the end of OGD with regular NB-A/B27 (ROG) and viability was assayed 15 h later.

After lifting, cell viability of SH-SY5Y was assessed by differential nuclear staining with Propidium Iodide (PI, live-cell impermeant red DNA dye) and Hoechst 33342 (cell permeant blue DNA dye) followed by quantitative flow cytometric analysis (FACSVantage SE flow cytometer) as described previously [37,38]. Due to their fragile nature, cell viability of cortical neurons was assessed by nuclear staining with PI and Hoechst 33342 performed directly in the well without lifting and the cells were counted manually under the fluorescent microscope, as previously described [35]. Cells were counted as follows: 10 fields were counted per sample. Each field had at least 200 cells. A total of 2000 cells/sample were counted. Experiments were conducted at least in triplicate.

Furthermore, as primary neuronal cultures do not readily lend themselves to prolonged and repeated manipulations, biochemical experiments were performed in the more adaptable neuroblastoma cell lines.

2.4. Western blot analysis

Total cell lysates or cytosol/nuclear fractions from SH-SY5Y cells were used for Western blot analysis (WB). Total cell lysates were prepared as described previously [35], and cytosolic or nuclear fractions were prepared following a previously reported protocol [39]. After protein concentrations were determined (BCA assay, Pierce), all samples were heated with ß-mercaptoethanol and dye (bromophenyl blue) for 5 min at 95 °C. Forty μg of total cell lysate and 10 μg of nuclear extract were used for each SDS-PAGE/WB analysis. The following primary antibodies were used for WB analyses: anti-PARP-1 (Cell Signaling Technology, Danvers, MA; Cat 9546S), anti-PARP-1 (N-20) (Santa Cruz Biotechnology, Santa Cruz, CA; Cat SC1561) to detect the 24 kDa fragment, anti-PARP-1 (C-2-10) (Biomol, Farmingdale, NY; Cat SA250), anti-PARs (Trevigen, Cat 4335-MC-100-AC), anti-p65 (Santa Cruz Biotechnology, Cat sc-372), anti-iNOS (Santa Cruz Biotechnology, Cat SC7221), anti-COX2 (Cayman, Cat 160126), anti-Bax (Cell Signaling Technology, Cat 2772), anti-Bcl-x_L (Cell Signaling Technology, Cat 2762), and anti-lamin (Abcam, Cat 16048-100). Signals were detected using a chemiluminescent substrate (Millipore) followed by digital imaging (Fluor Chem camera, Alpha Innotech, San Leandro, CA). The optical density of each western blot lane was measured using the software AlphaEaseFC 4.0.0. Data are expressed as percent of increase or decrease from control, after normalizing the density of each band by the density of the respective β-actin (total cell extracts) or lamin (nuclear extracts).

2.5. NAD^{+}/NADH quantification

Detection of total NAD (tNAD), NAD^+ and NADH, was performed using the NAD^+/NADH quantification kit (BioVision, San Francisco, CA). SH-SY5Y cells over-expressing PARP-1_{WT}, PARP-1_{UNCL}, PARP-1_{24} or PARP-1_{89} were seeded at a density of 7.5×10^5/well in a 6 well plate. Levels of tNAD were measured before and at the end of each OGD time period (30 min, 2 h, 6 h, 6 h + ROG 2 h, 6 h + ROG 4 h) in each group of cells. ROG was done to simulate "reperfusion" and restore levels of NAD, the PARP-1 substrate. Data were shown as percent of increase or decrease as compared to untreated cells expressing PARP-1_{WT}.

2.6. Caspase 3/7 activity assay

PARP-1 siRNA treated SH-SY5Y cells over-expressing PARP-1_{WT}, PARP-1_{UNCL}, PARP-1_{24} or PARP-1_{89} were transferred in a 96 well plate and subjected to 6 h OGD. Before and after OGD caspase 3/7 activity was measured (Apo 3/7 HTS; Cell Technology, Mountain View, CA). Results were expressed as percent of increase by OGD compared to control (without OGD) in each cell type.

2.7. Immunofluorescent staining of human SH-SY5Y cells

SH-SY5Y cells were seeded on chambered coverglass (Thermo Fisher Scientific, NY, Cat 155380) using DMEM complete with tet. The following day the medium was replaced with OGD medium and the cells were subjected to OGD for 10 min. Immunostaining was carried out using anti-p65 antibody (Santa Cruz Biotechnology, Cat sc-372) as a primary antibody and Alexa Fluor®488 (Molecular Probes) (in green) coupled goat anti-rabbit IgG as a second antibody. Nuclear staining (in blue) was performed using a mounting medium with DAPI (Vector Laboratories Inc., Burlingame, CA). Images were captured with an oil immersion 40× objective on a Zeiss LSM510 microscope using LSM Image Software.

2.8. Luciferase reporter assays: NF-kB and iNOS

Neuroblastoma cells expressing PARP-1_{WT}, PARP-1_{UNCL}, PARP-1_{24} or PARP-1_{89} were seeded in a 96-well plate 24 h before performing transfection for either NF-kB or *INOS* reporter plasmids. The NF-kB reporter assay was performed using the Cignal NFκB Reporter Assay Kit (SABiosciences, QIAGEN, Cat CCS-013L) following the manufacturer's instructions.

The *iNOS* reporter assay was performed using *INOS* WT (−1485/+31 NF-kB WT) and *INOS* mutant (−1485/+31 NF-kB mutant) constructs [40] (kind gift from Dr Mark Perrella). The mutant form of the *INOS* promoter region had been mutated such that NF-kB could not bind to it. NF-kB is, therefore, unable to bind to mutant *INOS* promoter, serving as a negative control of the NF-kB dependent *INOS* reporter assay. The *INOS* WT and mutant promoter regions in pGL2 vector (original constructs from Dr. Perrella) were transferred into a pGL4 vector (Promega) to enhance the firefly signal. These constructs (500 ng/well) were then co-transfected with renilla pRL-TK vector (100 ng/well) for the normalization of transfection efficiency. For both NF-kB and *INOS* assays, the measurements of firefly and renilla luciferase activities were performed at the end of 6 h of OGD using Dual-Glo Luciferase Assay System (Promega) and a luminometer (Centro LB 960, Berthold, Germany). Background subtraction and normalization were done for all experiments. NF-kB activity was expressed as percent of increase or decrease from control (PARP-1_{WT} before OGD).

2.9. RNA analyses by real-time polymerase chain reaction

Total RNA was isolated with the High Pure RNA Isolation kit (Roche Applied Science, Indianapolis, USA). Total RNA concentration was measured with NanoDrop 2000 UV–Vis Spectrophotometer (Thermo Fisher Scientific, DE, USA). 25 ng of RNA was used for real-time PCR analyses using the LightCycler LC480 System (Roche Applied Science, Indianapolis, USA) in a one step reaction using LightCycler 480 RNA Master Hydrolysis Probes. Primer pairs used (Real Time Ready from Roche Applied Science, Indianapolis, USA) and amplification protocol are listed in Supplementary Tables S1 and S2. We examined the gene expressions of *INOS* and *COX-2* (NF-kB-dependent genes) which have a kb-site located in their promoter regions. Samples were tested at least in duplicates. Gene specific expression was normalized to an endogenous control (Actin) and expressed in arbitrary units relative to the expression in untreated cells. Relative quantification was done using the standard curve method with PCR efficiency correction (E-method) of the LightCycler 480 Software (Roche). All samples were normalized to actin expression on the same plate. The relative mRNA level was calculated with the second derivative formula that corrects for PCR efficiency differences between target and reference gene [41].

2.10. Statistics

Data are shown as the mean ± SD. Statistical analyses were done by Student *T*-test and the number of experiments (n) is indicated in the figure legends. P values of $<0.05^{*}$, $<0.01^{**}$ and $<10^{-5***}$ were considered significant.

3. Results

3.1. Mutation from $DEVD_{214}$ to $DEVN_{214}$ renders PARP-1 resistant to caspase cleavage

PARP-1_{UNCL} was made by a point mutation (GAT → AAT) in the 214th codon of PARP-1_{WT}. As a result, the 214th amino acid of PARP-1_{WT}, an aspartate, was changed to an asparagine (D → N). This mutation makes PARP-1 uncleavable by activated caspases 3 and 7 (Fig. 1A).

Tet-inducible stable human SH-SY5Y transfectants were generated with PARP-1_{WT} or PARP-1_{UNCL}. As expected, PARP-1 protein (WT or UNCL) expression levels in these stable transfectants were significantly higher in the presence of tet (3.03-fold for PARP-1_{WT} and 2.94-fold for PARP-1_{UNCL}) compared to PARP-1 endogenous levels (cells grown without tet) (Fig. 1B, left and right panels). To confirm that PARP-1_{UNCL} would be resistant to caspases, the SH-SY5Y stable transfectants of PARP-1_{WT} or PARP-1_{UNCL} were grown with tet for 24 h and treated with 0.1 mM etoposide, a topoisomerase II inhibitor and a well known apoptosis-inducer, for 15 h. Cells were previously transiently transfected with siRNA-PARP-1. As shown in Fig. 1C, etoposide treatment caused PARP-1_{WT} cleavage and generated an 89 kDa fragment (53% of the available full length protein was cleaved) while PARP-1_{UNCL} was not cleaved as much by the same treatment, leaving the 116 kDa band mostly intact (only 22% of was cleaved, representing endogenous PARP-1 cleavage) ($n = 3$, $p < 0.02$). These findings indicate that the mutation at the DEVD site resulted in an uncleavable PARP-1, PARP-1_{UNCL}.

3.2. Overexpression of PARP-1_{UNCL} confers protection to SH-SY5Y cells from OGD-induced cell death

Since PARP-1_{UNCL} knock-in mice were reported to be more resistant to endotoxic shock or renal ischemia/reperfusion compared to WT [23], we tested whether human SH-SY5Y cells over-expressing PARP-1_{UNCL} were also more resistant to OGD compared to cells over-expressing PARP-1_{WT}. Unexpectedly, there was no difference in viability between cells over-expressing PARP-1_{WT} or PARP-1_{UNCL} after 15 h OGD. We suspected that endogenous PARP-1 might counteract any possible effect derived from overexpression of PARP-1_{UNCL}. To test this, endogenous PARP-1 was first depleted using siRNA-PARP-1. As shown in 2A, endogenous PARP-1 was almost completely depleted as compared to untreated cells as well as to cells treated with scrambled siRNA. We generated a new set of tet-inducible stable transfectants which were also siRNA resistant for PARP-1_{WT} or PARP-1_{UNCL}. Endogenous PARP-1 of these cells was almost completely depleted by 4 day-treatment of siRNA, and exogenous forms of PARP-1 were confirmed to be siRNA resistant (Fig. 2B). By simultaneous administration of siRNA and tet, exogenous PARP-1_{WT} or PARP-1_{UNCL} were exclusively expressed. Scramble siRNA was used for negative control (transfected in control cells). When these cells were challenged with OGD, PARP-1_{UNCL}-expressing cells were significantly more resistant compared to control cells (viability: 36.79 ± 4.7 control vs 62.32 ± 7.3; mean ± SD; $n = 8$; $p < 0.01$) (Fig. 2C; D bottom right panel). Additional controls were performed (data not shown) to make sure that, per se, the overexpression of PARP-1_{WT} or PARP-1_{UNCL}, siRNA or tet did not affect the viability of the cells. The results strongly suggest that PARP-1 cleavage or its cleavage products contribute to OGD-induced cell death. Without OGD, control cells (treated with siRNA scramble and not subjected to OGD showed a viability of 83.22 ± 0.67 for PARP-1_{WT} and 80.95 ± 2.32 for PARP-1_{UNCL} (Fig. 2C; D top panels)). That only cells expressing PARP-1_{UNCL} show a significantly higher viability

after OGD suggests that PARP-1 cleavage or its cleavage products might be involved in the regulation of OGD toxicity, and led us to take a closer look at how each cleavage product may contribute to this.

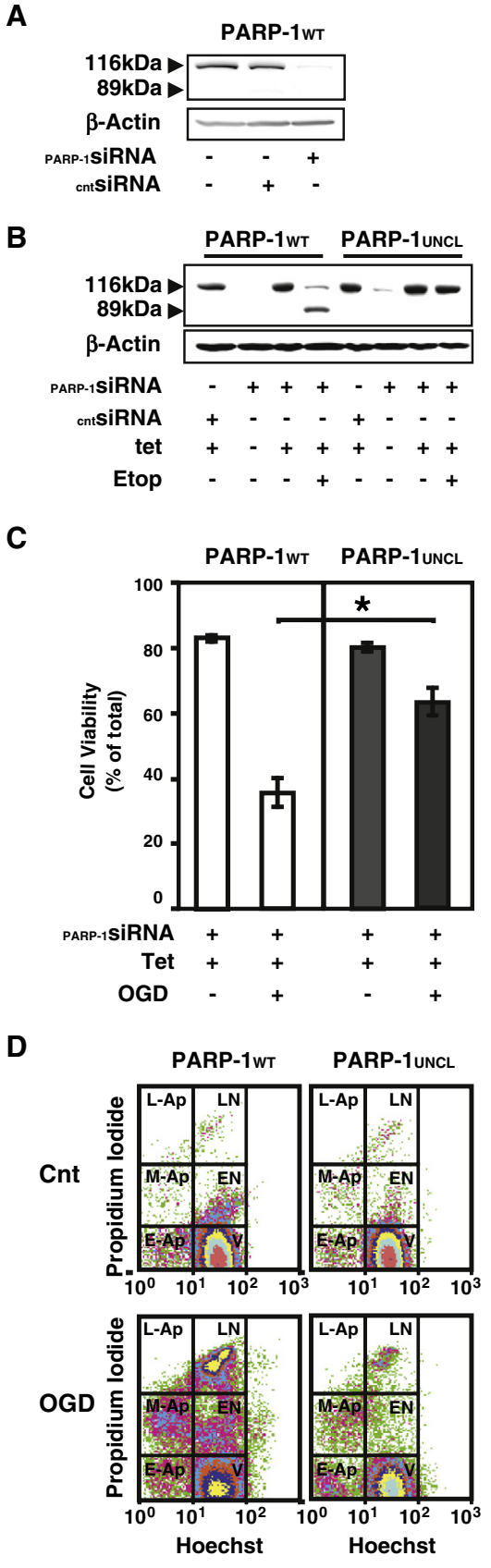

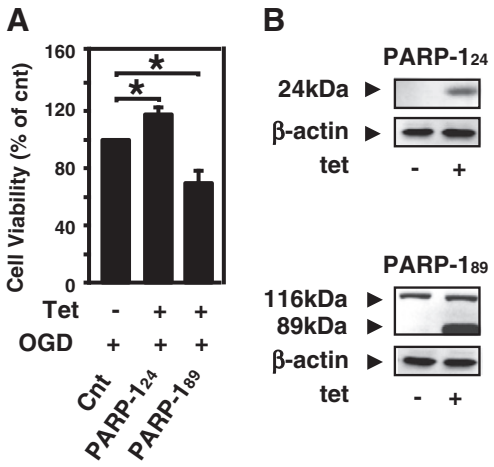

Fig. 3. Effects of PARP-1 cleavage products on OGD-induced cell death. (A) Viability of cells grown without tet (cnt = control), and PARP-1_{89} or PARP-1_{24} over-expressing cells (tet+) after 15 h OGD. Viable cell numbers were compared to non-tet control cells, calculated as percentage of control (without tet) cells, and shown as mean ± SD of at least 4 independent experiments (*$p < 0.05$). (B) Representative Western blots of nuclear fractions showing increased expression of PARP-1_{24} (top) and PARP-1_{89} (bottom). Cells were treated with siRNA before performing OGD.

3.3. SH-SY5Y cells over-expressing PARP-1_{24} show resistance to OGD while cells over-expressing PARP-1_{89} are more susceptible to cell death

Since PARP-1 cleavage is an event that results in the formation of two products at a ratio of 1:1, we examined the role of cleavage directly by using the cells that over-expressed each cleavage product (either PARP-1_{24} or PARP-1_{89}). When these cells were challenged by 15 h OGD, PARP-1_{24} conferred significant protection (18.09% increase in viability) compared to control cells ($n = 12$) ($p < 0.05$) (Fig. 3A). By contrast, PARP-1_{89} significantly decreased their viability, by 30.22%, when compared to control cells ($n = 3$) (Fig. 3A). Fig. 3B shows representative immunoblots of PARP-1_{24} (top panel) or PARP-1_{89} (bottom panel) expression levels with or without tetracycline. These data indicate that PARP-1 cleavage products have opposing effects on viability following OGD. PARP-1_{24} confers protection while PARP-1_{89} is harmful.

3.4. Primary rat cortical neurons transduced with PARP-1_{24} or PARP-1_{UNCL} are more resistant to OGD/ROG than neurons transduced with PARP-1_{WT}

Using conventional transfection methods, high transfection efficiency of primary cultures of rat cortical neurons is extremely hard to achieve. To overcome this, we developed a viral transduction method (see Materials and methods) that yields a transfection efficiency of approximately 60%. Due to their potential to confer protection in SH-SY5Y cells, we focused our efforts on PARP-1_{UNCL} and PARP-1_{24}. As

Fig. 2. Only after silencing endogenous PARP-1 does the over-expression of PARP-1_{UNCL} confer resistance to human SH-SY5Ycells exposed to 15 h OGD. (A) Western blots showing the depletion of endogenous PARP-1 by siRNA. Samples were total extracts from cells untreated (first lane), treated for 4 days with scrambled (negative control) (second lane) or treated with PARP-1 specific siRNA (third lane). (B) Western blots showing the depletion of endogenous PARP-1, the overexpression of siRNA resistant PARP-1_{WT} or PARP-1_{UNCL} and the defective accumulation of the 89 kDa fragment in PARP-1_{UNCL} overexpressing cells when etoposide was used. (C) Cell viability with or without 15 h OGD in siRNA-resistant PARP-1_{WT} (white bars) or PARP-1_{UNCL} (black bars) stable transfectants, with siRNA and tet. Data are shown as mean ± SD of 5 (for PARP-1_{WT}) or 8 (for PARP-1_{UNCL}) independent experiments (*$p < 0.01$). (D) Representative plots from flow cytometric analysis of Hoechst 33342 and PI labeled cells over-expressing PARP-1_{WT} (left) or PARP-1_{UNCL} (right) (tet +; siRNA+) before and after 15 h OGD. Most of the cells can be seen in the panel that depicts vital cells in the top panels (cells before OGD). A fewer number of apoptotic cells can be observed in the plot on the right corresponding to SH-SY5Y cells over-expressing PARP-1_{UNCL}. V = vital cells, M-Ap = middle apoptosis, L-Ap = late apoptosis, Vl-Ap = very late apoptosis, EN = early necrosis, LN = late necrosis. Cells were treated with siRNA before performing OGD.

shown in Fig. 4 (bottom panels and histogram), cortical neurons expressing PARP-1_{24} showed 51% increase in viability compared to cells expressing PARP-1_{WT} (PARP-1_{WT} = 100%, PARP-1_{24} = 151% ± 21.29; mean ± SD; n = 5 *T*-test, $p < 0.05$). Furthermore, cells expressing the uncleavable PARP-1_{UNCL} were 22% more viable compared to WT expressing cells (PARP-1_{WT} = 100%, PARP-1_{UNCL} = 121.75 ± 12; mean ± SD; n = 5 *T*-test, $p < 0.05$). Control cells (treated with the various viral constructs, but not challenged with OGD) (Fig. 4 top panels), all had comparable viabilities (67.52 ± 4.2 for PARP-1_{WT}, 65 ± 6.4 for PARP-1_{24}, 66 ± 3.8 for PARP-1_{UNCL}), suggesting that mere introduction of the virus did not disproportionately affect viability. These data both corroborate results from SH-SY5Y cells suggesting that PARP-1 cleavage may regulate cell viability, and also extend the findings to rat primary cultured neurons.

3.5. Changes in tNAD and PARs levels do not correlate with viability of SH-SY5Y cells over-expressing different forms of PARP-1 after OGD

PARP-1 enzymatic activity requires NAD as a substrate to form PARs, and it is possible that the observed differences in viability are due to the depletion/consumption of cellular NAD. Two approaches were used to assess PARylation: measurements of total NAD (tNAD) levels, and measurements of global PARs formation. These assays were performed in SH-SY5Y over-expressing PARP-1_{WT}, PARP-1_{UNCL}, PARP-1_{24} or PARP-1_{89} untreated and exposed to 30 min, 2 h, 6 h OGD, 6 h OGD + 2 h ROG and 6 h OGD + 4 h ROG. H_2O_2 (200 μM for 1 h) was used as a positive control since it is known to induce DNA strand breaks and, as a consequence, PARP-1 activation (PARylation) that in turn consumes tNAD. Levels of tNAD significantly decreased in each cell group after 6 h OGD when compared to tNAD levels measured before OGD (Fig. 5A; white vs red bars). It is interesting to note that the baseline tNAD level for PARP-1_{89} is lower than PARP-1_{WT}, PARP-1_{UNCL}, or PARP-1_{24} ($p < 0.01$ vs WT). However, with the same OGD or OGD/ROG treatment there was no significant difference among cells expressing the different forms of PARP-1 (Fig. 5A; colored bars). Similarly, levels of tNAD greatly decreased after H_2O_2 treatment, as expected, and no difference was found among these groups (Fig. 5A; green bars).

To address the possibility that parallel changes in PARs levels contributed to the differences in viability, PARs formation was evaluated at the time periods of 30 min and 6 h OGD, based on a pilot time course study. A significant increase in PARs levels was observed following 30 min OGD for all PARP-1 constructs, except PARP-1_{89} (Fig. 5B). Baseline PARs levels for PARP-1_{89} were already elevated as compared to the other three forms of PARP-1, an observation complementing that seen for tNAD levels (Fig. 5B). In contrast, PARs levels detected after 6 h OGD were comparable and not significantly different across all groups (PARP-1_{WT}, PARP-1_{UNCL}, PARP-1_{24} or PARP-1_{89}) (Fig. 5C).

These findings suggest that PARylation (PARs formation and tNAD) may not have a role in the regulation of PARP-1 and NF-kB activity observed in this system.

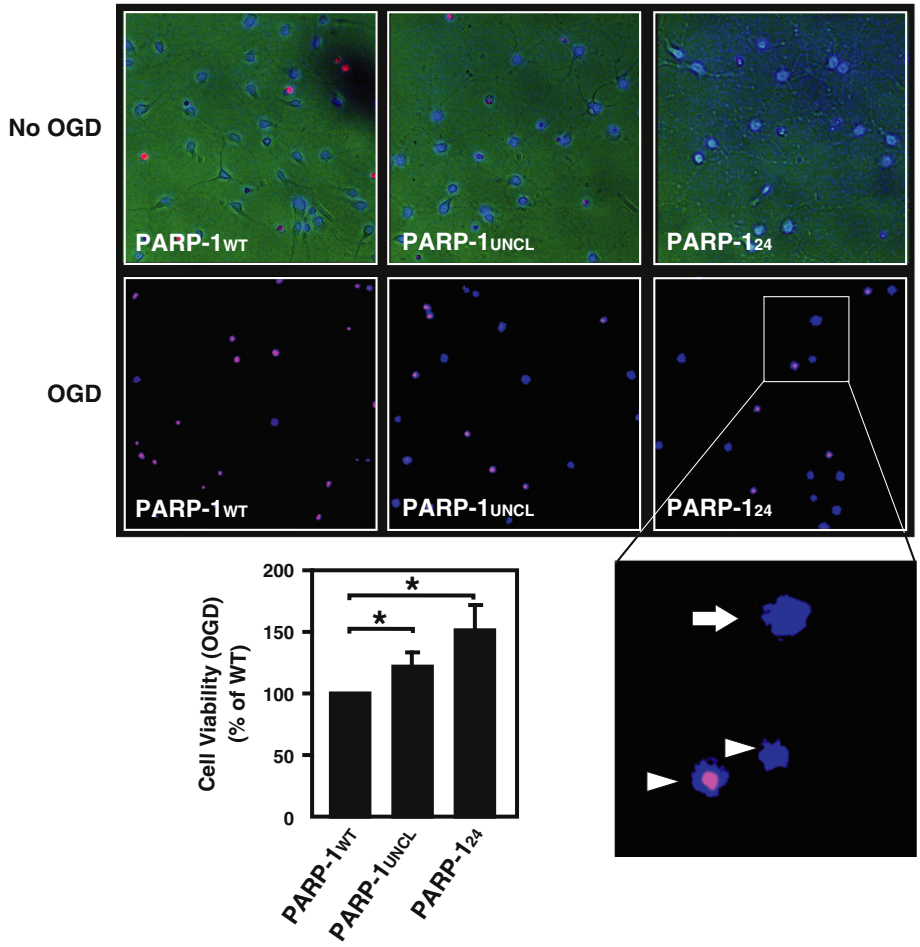

Fig. 4. Primary cortical neurons from rat over-expressing PARP-1_{24} or PARP-1_{UNCL} were more resistant to OGD/ROG compared to WT. Panels labeled "No OGD" show representative bright field, Hoechst 33342 and PI fluorescence images of PARP-1_{WT}, PARP-1_{UNCL} or PARP-1_{24} over-expressing cortical neurons before OGD/ROG. Panels labeled "OGD" show representative Hoechst 33342 and PI fluorescence images of PARP-1_{WT}, PARP-1_{UNCL} or PARP-1_{24} over-expressing cortical neurons after 6 h of OGD followed by 15 h of reperfusion (ROG). Cell viability in each cell preparation was quantitated and shown in the graph on the bottom left. The inset shows representative examples of a vital cell (diffuse blue nucleus with no PI staining, top arrow), early apoptotic cell (pyknotic blue nucleus with no PI staining, top arrowhead) or late apoptotic/necrotic cell (pyknotic blue nucleus with bright red PI staining, bottom arrowhead). Data are shown as mean ± SD of 5 independent experiments (*$p < 0.05$).

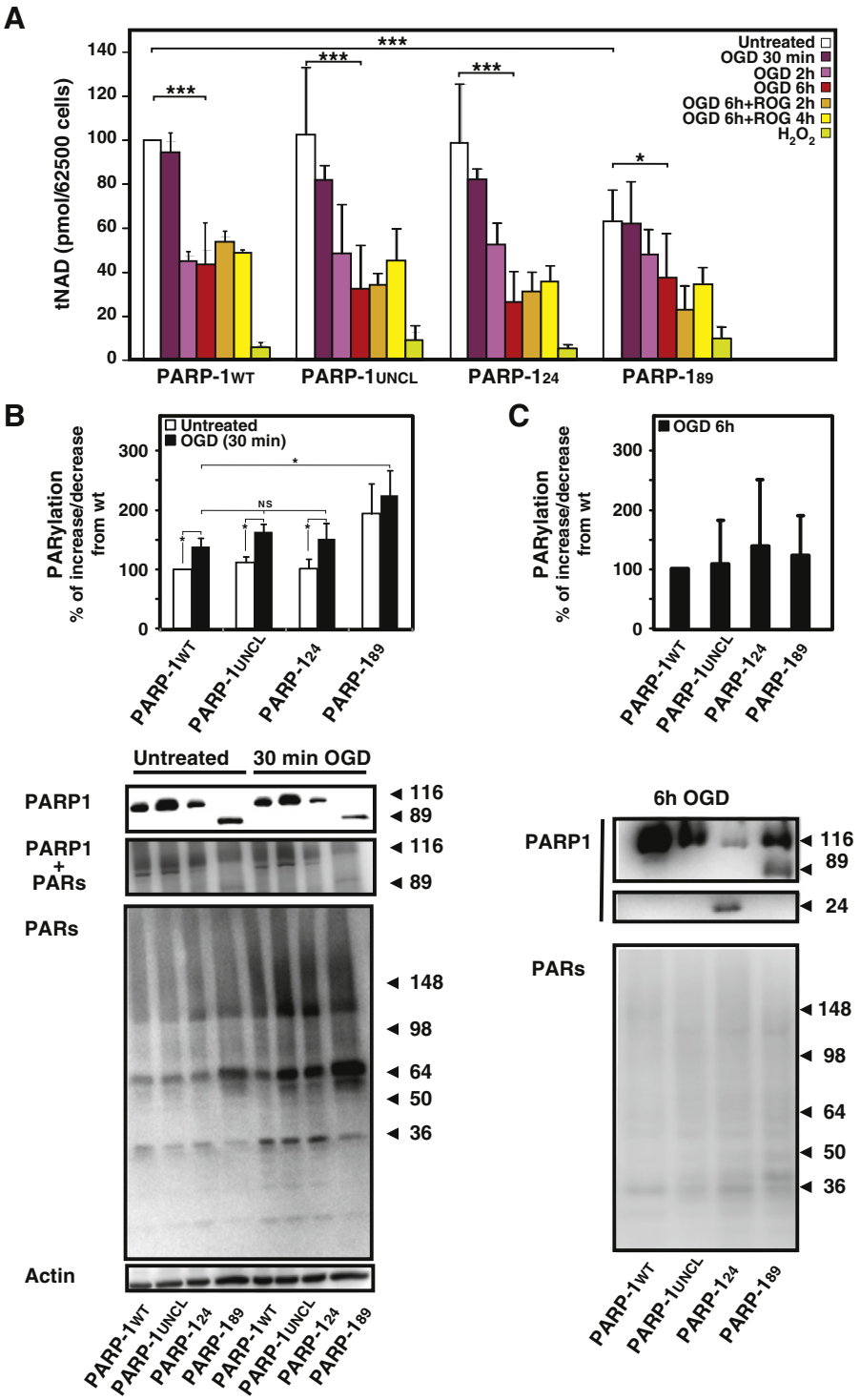

Fig. 5. Total NAD consumption and PARs formation levels in SH-SY5Y cells over-expressing PARP-1_{WT}, PARP-1_{UNCL}, PARP-1_{24} or PARP-1_{89} after different time points of OGD and OGD/ROG. (A) Quantitative analyses of the levels of tNAD. Data are shown as mean ± SD (n = 12). $p < 0.05^{*}$; $p < 10^{-5***}$. (B) Relative PARylation levels among cells after 30 min OGD. Quantification of Western blot densitometry of n = 3 (top panel); Western blot in the lower panel. (C) Relative PARylation levels among cells after 6 h OGD. Quantification of Western blot densitometry of n = 5 (top panel); Western blot in the lower panel. OGD = oxygen and glucose deprivation; ROG = restoration of oxygen and glucose; NS = not significant. Cells were treated with siRNA before performing OGD.

3.6. OGD or OGD/ROG treatment induces caspase activation and PARP-1 cleavage

The appearance of the 89 kDa fragment has been considered as a hallmark for apoptosis [16] and the occurrence of PARP-1 cleavage in ischemia models has been shown before [42,43]. In our model, the fragment was indeed seen in SH-SY5Y cells subjected to a prolonged OGD (15 h) (Fig. S1 A) and in cortical neurons after 2–4 h OGD followed by 15 h ROG (Fig. S1 C). The lack of the appearance of 89 kDa fragment in earlier OGD time points (data not shown) might be a reflection of the limit of the Western blot assay sensitivity, since caspases 3 and 7 which are responsible for PARP-1 cleavage were already activated as early as 6 h OGD (Fig. S1 B). However, no differential activations were seen among cells over-expressing PARP-1_{WT}, PARP-1_{UNCL}, PARP-1_{24} or

PARP-1_{89} at least at this time point; an increase of caspase 3/7 activity that varied around 30% was observed in all cell types (Fig. S1 B). These results suggest that the protective effects found in PARP-1_{UNCL} and PARP-1_{24} cells were from downstream events.

3.7. PARP-1 cleavage and its cleavage products do not influence nuclear translocation of NF-kB induced by OGD

Since cell sensitivity to OGD seems not to depend on PARylation, we next examined the possibility that another function of PARP-1, a cofactor for NF-kB, plays a role in cell viability during OGD. To do so, we first examined the initial step of NF-kB activation, namely p65 (a subunit of NF-kB) translocation into the nucleus. In primary cortical neurons from rats, nuclear levels of p65 increase by 30 min after OGD, peak at 2 h and decrease to baseline by 4 h (Fig. 6 A). While levels of p65 increased in the nucleus by 2 h in cortical neurons from rats, a corresponding decrease in p65 cytoplasmic levels was difficult to observe. However, IKB-α, the protein that anchors p65 in the cytoplasm, is degraded at 2–4 h of OGD (Fig. S2). Human SH-SY5Y cells showed p65 nuclear translocation within 10 min of OGD in the all of the cell types examined (e.g. expressing PARP-1_{WT}, PARP-1_{UNCL}, PARP-1_{24} or PARP-1_{89}) (Figs. 6B and S3). From these results it is clear that OGD is indeed a stimulus that induces NF-kB nuclear translocation, but this action was not affected by PARP-1 cleavage or cleavage products.

3.8. PARP-1 cleavage appears to be a regulator of NF-kB activity in SH-SY5Y

PARP-1 and NF-kB are known to be part of a larger nuclear multiprotein complex involved in gene transcription [11,44]. We hypothesized that PARP-1 cleavage products may differentially regulate activity of NF-kB once it is in the nucleus. To test this hypothesis we used a NF-kB reporter assay to evaluate global NF-kB activity. OGD induced NF-kB activity comparably in all cell groups except PARP-1_{89} cells, which displayed a significant increase (Fig. 7A). We then analyzed a well known NF-kB-dependent gene, *INOS*. To study the specificity of NF-kB p65 subunit binding to *INOS* promoter, we used two constructs: one was WT for *INOS* promoter region [*INOS*(−1485/+31 NF-κB WT)] and the other was mutated at 3 binding sites of NF-κB for *INOS* promoter region [*INOS*(−1485/+31 NF-κB mut)]. The mutant form of the *INOS* promoter had been mutated such that NF-kB could not bind to it. For this reason, it can be used as a negative control to investigate the dependency of NF-kB activity in *INOS* reporter assays. OGD increased the levels of p65-dependent *INOS* transcription in all cell types. Among them, cells expressing PARP-1_{89} showed a significantly greater increase of *INOS* transcription than the other PARP-1 isoforms (Fig. 7B). This increase was specifically induced by NF-kB since there was no corresponding increase in the levels of *INOS* expression when the *INOS* mutant construct was used (Fig. 7B), suggesting that PARP-1_{89} indeed modulates NF-kB activity.

To confirm these data, rt-qPCR was used. First a time course for OGD was performed and a peak in expression level for both *INOS* and *COX-2* was identified at 4 h (Fig. 7C). Next, SH-SY5Y cells overexpressing PARP-1_{WT}, PARP-1_{UNCL}, PARP-1_{24} or PARP-1_{89} were subjected to 4 h OGD and the levels of *INOS* transcript confirmed the data obtained by the reporter assay (Fig. 7D). In particular, *INOS* message level is significantly higher in the cells expressing PARP-1_{89} and significantly lower in PARP-1_{24} expressing cells compared to PARP-1_{WT} expressing cells.

3.9. Cells over-expressing PARP-1_{UNCL} or PARP-1_{24} which are protected from OGD show a reduced inflammatory profile

In order to estimate the scope of the effect of PARP-1 cleavage products, particularly the 89 kDa fragment on NF-kB activity, we chose several proteins with NF-kB-dependent expression such as MnSOD, ICAM-1, c-IAP, MMP-9, iNOS, COX-2, Bax and Bcl-x_L and analyzed them in human SH-SY5Y cells expressing PARP-1_{WT}, PARP-1_{UNCL}, PARP-1_{24} or PARP-1_{89}. SH-SY5Y cells were subjected to 6 h OGD and the levels of the proteins mentioned above were measured by Western blot analyses. Among them, we found the protein expressions of iNOS, COX-2, Bax and Bcl-x_L were influenced by PARP-1_{UNCL} or PARP-1 products. The pro-inflammatory/harmful protein iNOS (Fig. 8A, white bars) which is known to have a kb-site located in its promoter, was significantly lower in cells over-expressing either PARP-1_{24} or PARP-1_{UNCL} by 46% and 33%, respectively ($n = 3$; $p < 0.05$), compared to WT cells after 6 h OGD. COX-2 protein levels in these cells were comparable to WT cells. In contrast, the expression of an anti-apoptotic/protective protein Bcl-x_L was significantly higher in these cells (twice as much in PARP-1_{24} expressing cells compared to PARP-1_{WT}, $n = 5$, $p < 0.05$) (Fig. 8B, light gray). These data support the idea that the protection conferred by the over-expression of PARP-1_{24} and uncleavable PARP-1_{UNCL} could be mediated, in part, through NF-kB regulation of iNOS (down regulation), COX-2 (no increase observed) and Bcl-x_L (up regulation). Conversely, cells over-expressing PARP-1_{89}, which were very sensitive to OGD, showed a significantly higher level of the pro-inflammatory/harmful proteins iNOS and COX-2 (1.7-fold, $n = 3$, $p < 0.05$) and lower level of Bcl-x_L (58% of WT, paired *t*-test; $p < 0.05$). Finally, even if the expression levels of pro-apoptotic protein Bax were not significantly different among these cell groups, there is a reduction in its levels in cells expressing PARP-1_{UNCL} and PARP-1_{24}.

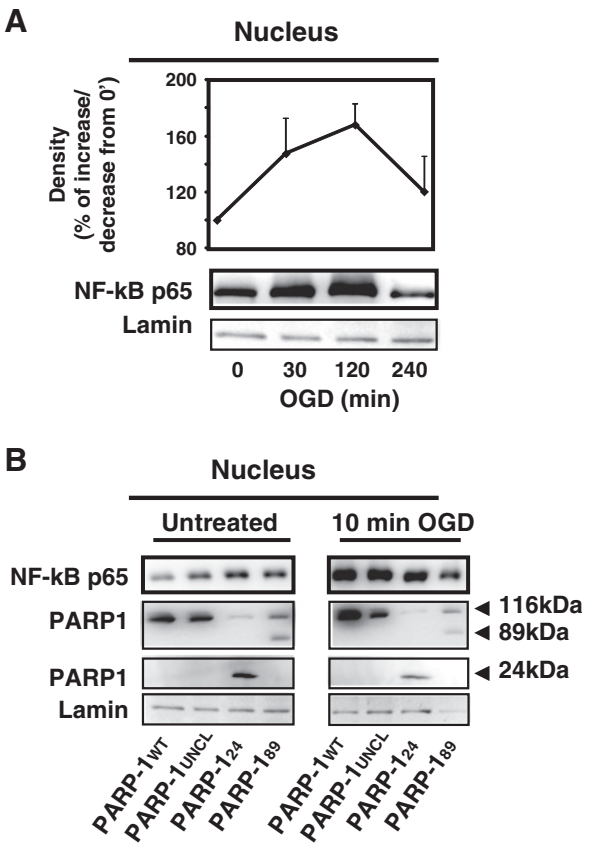

Fig. 6. OGD induces NF-kB translocation to the nucleus. (A) Primary rat cortical neurons were exposed to OGD for 0, 30, 120 and 240 min. Nuclear levels of NF-kB p65 subunit were analyzed by Western blot ($n = 3$) (B) The nuclear translocation of p65 was apparent by 10 min of OGD in human SH-SY5Y cells expressing PARP-1_{WT}, PARP-1_{UNCL}, PARP-1_{24} or PARP-1_{89}. Representative blot is shown. Cells were treated with siRNA before performing OGD.

4. Discussion

This report sheds light on the functional role of PARP-1 cleavage products in models of in vitro "ischemia" using OGD in human SH-SY5Y cells and OGD/ROG in primary rat cortical neurons. To the best

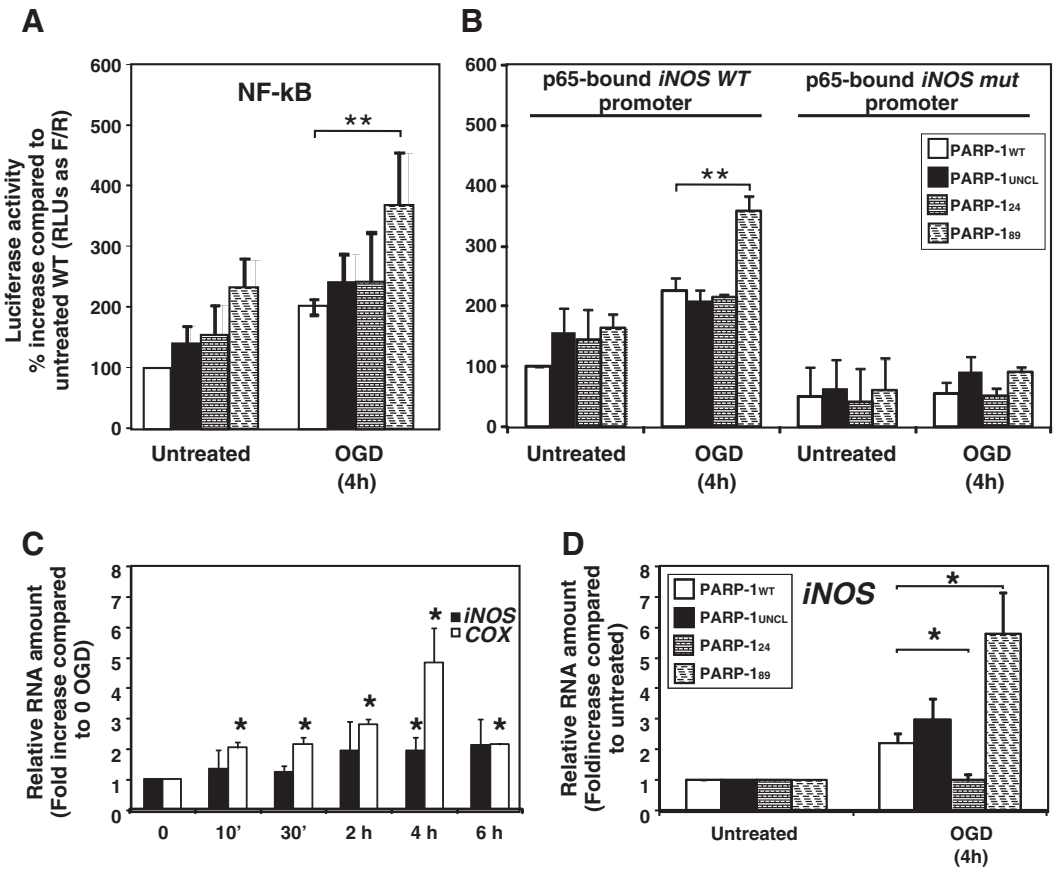

Fig. 7. NF-kB and iNOS reporter assays. OGD (4 h) induces an increase in NF-kB and iNOS activity in human SH-SY5Y expressing PARP-1_{WT}, PARP-1_{UNCL}, PARP-1_{24} or PARP-1_{89}. (A) Though the increase in NF-kB activity can be observed in all cell groups after OGD, among these cells only PARP-1_{89} induced a significantly higher activity compared to PARP-1_{WT}, PARP-1_{UNCL} or PARP-1_{24}. (B) When the construct for *INOS* promoter used was WT for NF-kB binding sites (*INOS* WT), OGD induced an increase in *INOS* activity in cells expressing PARP-1_{WT}, PARP-1_{UNCL}, PARP-1_{24} and PARP-1_{89}. Among these cells only PARP-1_{89} showed a significant increase in *INOS* transactivation. When the construct for iNOS promoter used was mutated for NF-kB binding sites (*INOS* mut) none of the cells showed an induction of the signal with OGD, suggesting that PARP-1 acts through NF-KB transactivation. All reporter assay experiments were conducted in the presence of siRNA, in triplicates, repeated at least 3 independent times and conducted at the same time for the different cell lines; $p < 0.01$. RLUs as F/R = Relative luciferase units as firefly/renilla. Fig. 7C and D provides quantitative analyses of transcription levels for *iNOS* and *COX-2* during OGD. (C) Levels of *iNOS* and *COX-2* transcripts measured after OGD in wild type SH-SY5Y cells (time course). (D) Levels of *INOS* RNA after 4 h OGD in cells overexpressing PARP-1_{WT}, PARP-1_{UNCL}, PARP-1_{24}, and PARP-1_{89}. Cells were pretreated with siRNA. Results are expressed as mean ± SD of n = 3.

of our knowledge, this is the first study demonstrating that expression of the uncleavable PARP-1_{UNCL} confers protection in this model. It is interesting that even though PARP-1_{UNCL} is not present in nature, our findings and previous studies [23,45] suggest that PARP-1 cleavage and its cleavage products regulate functions and control mechanisms related to cell survival and cell death. Hence, a novel element in this study was to show differential effects on viability by the 24 kDa and the 89 kDa fragment, products of PARP-1 cleavage.

This study also reports that the overexpression of PARP-1_{24} confers protection from OGD in SH-SY5Y cells as well from OGD/ROG in cortical neurons, suggesting that this part of the molecule may be necessary to perform this function. PARP-1_{24} preserves more than 60% of the PARP-1 DNA binding domain; it has been shown that this fragment may compete with PARP-1_{WT} for DNA binding and reduce PARylation [17,46–48]. If this were occurring in our studies, one would expect to see higher levels of NAD and lower levels of PARylation after OGD compared to WT in cells expressing this fragment. However, PARP-1_{24} (like PARP-1_{UNCL}) did not change NAD levels and PARylation after OGD. As cellular apoptosis was also not apparent, we evaluated the hypothesis that PARP-1 cleavage products might affect NF-kB-dependent molecular pathways.

It has been shown that PARP-1 can bind to NF-kB [11], and that subsequent PARP-1 cleavage by caspases 3 and 7 could modulate the NF-kB-dependent inflammatory response in an apoptosis-independent event [20,23,45]. We then hypothesized that PARP-1 cleavage could be an element that finely tunes NF-kB activity, depending on its binding to different parts of the PARP-1 molecule (N or C-terminal fragment), which are produced by the cleavage (hypothetical model in Fig. 9). Although it is still unclear in our system whether the influence of PARP-1 fragments on NF-kB is indirect or occurs via direct interaction, several differences in NF-kB activity and NF-kB-related molecules were seen when the different constructs were expressed in SH-SY5Y. In our model, OGD induces p65 translocation into the nucleus in both cell types within 10 min. "Ischemia" in vitro increases NF-kB global activity in all groups, but no further increase was observed for either PARP-1_{UNCL} or PARP-1_{24} overexpressing cells. In contrast, cells expressing PARP-1_{89} show a significant increase in both general NF-kB activity as well as NF-kB-dependent induction of *iNOS*. In addition, cleaved fragments PARP-1_{24} and PARP-1_{89} have opposing actions on the protein levels of reported NF-kB downstream effectors iNOS (as well as on increased *iNOS* transcript levels), COX-2, and Bcl-$_{XL}$. Collectively, these data suggest that even though there is an increase in NF-kB activity, this increase could be translated into either an increase or a decrease in molecules usually considered markers of a more "anti-inflammatory" or "pro-inflammatory" profile. It should be noted that, although neuroblastoma cells are not classically considered

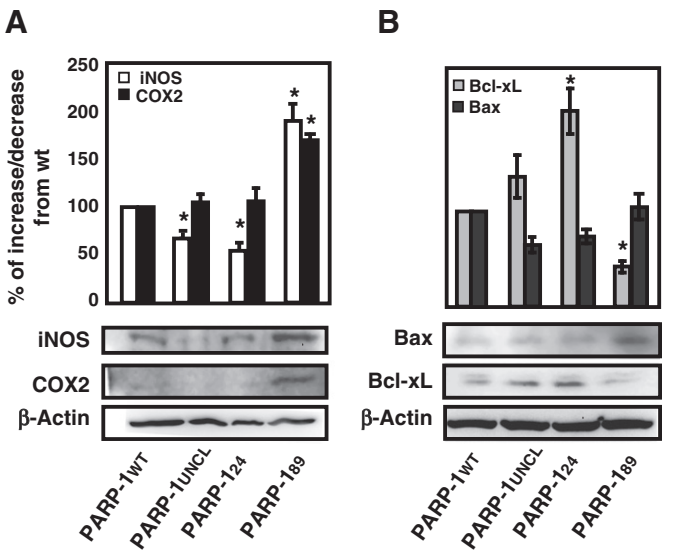

Fig. 8. Quantitative analyses of protein expression levels of iNOS, COX-2, Bcl-x_L and Bax in cells over-expressing PARP-1_{WT}, PARP-1_{UNCL}, PARP-1_{24} or PARP-1_{89} after 6 h OGD. Bottom panels are representative Western blots. The densities of each protein band, from total cell extracts, were measured and normalized with corresponding actin levels and expressed as percentage of that of PARP-1_{WT} cells. (A) Levels of pro-inflammatory/harmful proteins iNOS and COX2. (B) Levels of anti-apoptotic/protective Bcl-x_L and pro-apoptotic Bax. Data are shown as mean ± SD of four independent experiments (*$p < 0.05$). Cells were transiently transfected with siRNA.

inflammatory cells, they have been associated with changes in molecules involved in inflammatory pathways [49,50]. We demonstrated that the overexpression of PARP-1_{UNCL} as well as PARP-1_{24} is associated with decreases in iNOS and COX-2 proteins, and an upregulation of the anti-apoptotic/protective protein Bcl-x_L. The expression of these proteins suggests that these anti-inflammatory events may be, at least in part, NF-kB-dependent and are supported by findings in the literature [51–53]. In addition, the results of the present study demonstrate that PARP-1_{89}, the other product of PARP-1 cleavage, appears to alter NF-kB transactivation towards a pro-inflammatory profile.

These observations support the idea that an increase of C-terminal PARP-1_{89} enhances the toxicity of OGD. Previous studies suggested that the role of PARP-1 cleavage is to protect the cell by inactivation of PARylation and NAD depletion, and others have reported a loss of PARP-1 enzymatic activity after cleavage [17]. It is possible that a reduction in the levels of NAD combined with the increased PARs in the PARP-1_{89} cells may contribute to an increased energy imbalance, which could partially explain the increased toxicity seen when this construct is expressed. However, several contradictory observations bring this inference into question. First, levels of NAD are the same across all the cell lines following OGD (Fig. 5A). If NAD were a factor, one would expect the levels seen with PARP-1_{89} to be much lower following OGD. Second, NAD levels in the protected cells (PARP-1_{UNCL} and PARP-1_{24}) are not higher than the control (PARP-1_{WT}). Following p65 nuclear translocation, we observed a significant increase in global NF-kB activity when compared to PARP-1_{WT} as well as a significant increase in NF-kB-dependent *iNOS* activity. Furthermore, these changes

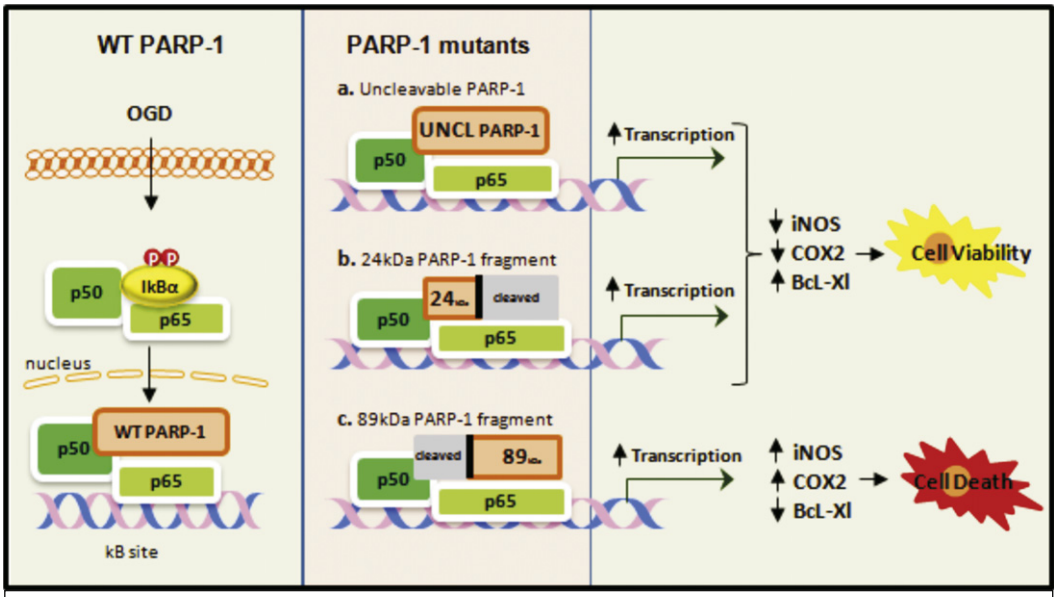

Green areas (left and right) indicate events that have been investigated in this study. The formation of the multiprotein complex between NF-kB (p65+p50) is a known phenomenon in the literature (see ref).
The orange area in the middle represents a hypothetical mechanism that might explain the differential expression of downstream effectors of NF-kB and cell viability.

Fig. 9. Hypothetical model of the mechanism of action of PARP-1 and its cleavage products. Green areas (left and right) indicate events that have been investigated in this study. The formation of the multiprotein complex between PARP-1 and NF-kB (p65+p50) is a known phenomenon in the literature (see Refs. [11,20,56,57]). The orange area in the middle represents a hypothetical mechanism that might explain the differential expression of downstream effectors of NF-kB and cell viability. Upon stimulation with OGD, NF-kB translocates into the nucleus where PARP-1 acts as its co-modulator, modifying *NF-kB* gene transactivation (left side). NF-kB increased activity is observed when each of the PARP-1 constructs (PARP-1_{UNCL}, PARP-1_{24} or PARP-1_{89}) is expressed (right side). The findings in this study suggest that NF-kB increased activity is not only a quantitative phenomenon during cellular ischemic stress, but also a finely tuned event perhaps influenced by co-factors such as PARP-1. PARP-1 and its cleavage products may be capable of regulating post-translational events depending on which part of the PARP-1 molecule is regulating NF-kB activity. After OGD, the expression of PARP-1_{UNCL} or PARP-1_{24} (a and b) leads to an increased NF-kB activity in a more anti-inflammatory/protective fashion (decreased iNOS and COX-2 protein levels; increased Bcl-x_L). The expression of PARP-1_{89} also induces NF-kB transactivation, but its downstream effectors (iNOS and COX-2 increased; Bcl-x_L decreased) show a more pro-inflammatory profile (c.). NF-kB = p65 + p50; 24 kDa = PARP-1_{24}; 89 kDa = PARP-1_{89}.

were accompanied by higher levels of the pro-inflammatory/harmful protein iNOS (as well as its mRNA), COX-2 and the amount of the anti-apoptotic/protective protein Bcl-x_L.

These observations provide renewed impetus for further investigation of the mechanisms involved in NF-kB regulation —a transcription factor with well known clinical significance. The findings provide just one paradigm of the complex protein regulation in which PARP-1 is just one of the players. However, understanding how the intricate protein to protein interactomes [44,54,55] are regulated is an important, if daunting challenge.

Supplementary data to this article can be found online at http://dx.doi.org/10.1016/j.bbamcr.2013.12.005.

Acknowledgements

This research was supported by the Intramural Research Program of the NIH, NINDS/NIH. No conflict of interest to disclose.

The authors are particularly thankful to Dace Klimanis for technical assistance. We would like to thank Debbie Kauffman and James W. Nagle at the NINDS DNA sequencing facility, as well as Carolyn Smith and Paul Gallant at the NINDS Confocal facility. We would like to acknowledge the Harvard Institute of Proteomics for sharing PARP-1_{WT} plasmid. We are very grateful to Dr Mark Perrella for sharing with us the *iNOS*(−1485/+31 NF-kB mutant) and *iNOS*(−1485/+31 NF-kB WT) constructs.

References

[1] M.O. Hottiger, P.O. Hassa, B. Luscher, H. Schuler, F. Koch-Nolte, Toward a unified nomenclature for mammalian ADP-ribosyltransferases, Trends Biochem. Sci. 35 (2010) 208–219.
[2] D. D'Amours, S. Desnoyers, I. D'Silva, G.G. Poirier, Poly(ADP-ribosyl)ation reactions in the regulation of nuclear functions, Biochem. J. 342 (Pt 2) (1999) 249–268.
[3] J. Infante, P. Sanchez-Juan, I. Mateo, E. Rodriguez-Rodriguez, C. Sanchez-Quintana, J. Llorca, A. Fontalba, J. Terrazas, A. Oterino, J. Berciano, O. Combarros, Poly (ADP-ribose) polymerase-1 (PARP-1) genetic variants are protective against Parkinson's disease, J. Neurol. Sci. 256 (2007) 68–70.
[4] S.S. Kassner, G.A. Bonaterra, E. Kaiser, W. Hildebrandt, J. Metz, J. Schroder, R. Kinscherf, Novel systemic markers for patients with Alzheimer disease? —a pilot study, Curr. Alzheimer Res. 5 (2008) 358–366.
[5] V. Selvaraj, M.M. Soundarapandian, O. Chechneva, A.J. Williams, M.K. Sidorov, A.M. Soulika, D.E. Pleasure, W. Deng, PARP-1 deficiency increases the severity of disease in a mouse model of multiple sclerosis, J. Biol. Chem. 284 (2009) 26070–26084.
[6] A.M. Hamby, S.W. Suh, T.M. Kauppinen, R.A. Swanson, Use of a poly(ADP-ribose) polymerase inhibitor to suppress inflammation and neuronal death after cerebral ischemia–reperfusion, Stroke 38 (2007) 632–636.
[7] T.M. Kauppinen, Multiple roles for poly(ADP-ribose)polymerase-1 in neurological disease, Neurochem. Int. 50 (2007) 954–958.
[8] O. Hayaishi, K. Ueda, Poly(ADP-ribose) and ADP-ribosylation of proteins, Annu. Rev. Biochem. 46 (1977) 95–116.
[9] R. Krishnakumar, W.L. Kraus, The PARP side of the nucleus: molecular actions, physiological outcomes, and clinical targets, Mol. Cell 39 8-24.
[10] R. Aguilar-Quesada, J.A. Munoz-Gamez, D. Martin-Oliva, A. Peralta-Leal, R. Quiles-Perez, J.M. Rodriguez-Vargas, M.R. de Almodovar, C. Conde, A. Ruiz-Extremera, F.J. Oliver, Modulation of transcription by PARP-1: consequences in carcinogenesis and inflammation, Curr. Med. Chem. 14 (2007) 1179–1187.
[11] P.O. Hassa, C. Buerki, C. Lombardi, R. Imhof, M.O. Hottiger, Transcriptional coactivation of nuclear factor-kappaB-dependent gene expression by p300 is regulated by poly(ADP)-ribose polymerase-1, J. Biol. Chem. 278 (2003) 45145–45153.
[12] Z.Y. Abd Elmageed, A.S. Naura, Y. Errami, M. Zerfaoui, The poly(ADP-ribose) polymerases (PARPs): new roles in intracellular transport, Cell. Signal. 24 1-8
[13] J. Krietsch, M. Rouleau, E. Pic, C. Ethier, T.M. Dawson, V.L. Dawson, J.Y. Masson, G.G. Poirier, J.P. Gagne, Reprogramming cellular events by poly(ADP-ribose)-binding proteins, Mol. Aspects Med. 34 1066-1087.
[14] S. Smith, The world according to PARP, Trends Biochem. Sci. 26 (2001) 174–179.
[15] M.F. Langelier, K.M. Servent, E.E. Rogers, J.M. Pascal, A third zinc-binding domain of human poly(ADP-ribose) polymerase-1 coordinates DNA-dependent enzyme activation, J. Biol. Chem. 283 (2008) 4105–4114.
[16] C. Soldani, A.I. Scovassi, Poly(ADP-ribose) polymerase-1 cleavage during apoptosis: an update, Apoptosis 7 (2002) 321–328.
[17] D. D'Amours, F.R. Sallmann, V.M. Dixit, G.G. Poirier, Gain-of-function of poly(ADP-ribose) polymerase-1 upon cleavage by apoptotic proteases: implications for apoptosis, J. Cell Sci. 114 (2001) 3771–3778.
[18] Z. Herceg, Z.Q. Wang, Functions of poly(ADP-ribose) polymerase (PARP) in DNA repair, genomic integrity and cell death, Mutat. Res. 477 (2001) 97–110.
[19] W.J. Chang, R. Alvarez-Gonzalez, The sequence-specific DNA binding of NF-kappa B is reversibly regulated by the automodification reaction of poly (ADP-ribose) polymerase 1, J. Biol. Chem. 276 (2001) 47664–47670.
[20] M. Lamkanfi, W. Declercq, T. Vanden Berghe, P. Vandenabeele, Caspases leave the beaten track: caspase-mediated activation of NF-kappaB, J. Cell Biol. 173 (2006) 165–171.
[21] P.O. Hassa, M. Covic, M.T. Bedford, M.O. Hottiger, Protein arginine methyltransferase 1 coactivates NF-kappaB-dependent gene expression synergistically with CARM1 and PARP1, J. Mol. Biol. 377 (2008) 668–678.
[22] F.J. Oliver, J. Menissier-de Murcia, C. Nacci, P. Decker, R. Andriantsitohaina, S. Muller, G. de la Rubia, J.C. Stoclet, G. de Murcia, Resistance to endotoxic shock as a consequence of defective NF-kappaB activation in poly (ADP-ribose) polymerase-1 deficient mice, EMBO J. 18 (1999) 4446–4454.
[23] V. Petrilli, Z. Herceg, P.O. Hassa, N.S. Patel, R. Di Paola, U. Cortes, L. Dugo, H.M. Filipe, C. Thiemermann, M.O. Hottiger, S. Cuzzocrea, Z.Q. Wang, Noncleavable poly(ADP-ribose) polymerase-1 regulates the inflammation response in mice, J. Clin. Invest. 114 (2004) 1072–1081.
[24] A.S. Baldwin Jr., The NF-kappa B and I kappa B proteins: new discoveries and insights, Annu. Rev. Immunol. 14 (1996) 649–683.
[25] Q. Wang, M. van Hoecke, X.N. Tang, H. Lee, Z. Zheng, R.A. Swanson, M.A. Yenari, Pyruvate protects against experimental stroke via an anti-inflammatory mechanism, Neurobiol. Dis. 36 (2009) 223–231.
[26] J. Aronowski, R. Strong, H.S. Kang, J.C. Grotta, Selective up-regulation of I kappaB-alpha in ischemic penumbra following focal cerebral ischemia, Neuroreport 11 (2000) 1529–1533.
[27] Q. Li, I.M. Verma, NF-kappaB regulation in the immune system, Nat. Rev. Immunol. 2 (2002) 725–734.
[28] T.M. Kauppinen, S.W. Suh, A.E. Berman, A.M. Hamby, R.A. Swanson, Inhibition of poly(ADP-ribose) polymerase suppresses inflammation and promotes recovery after ischemic injury, J. Cereb. Blood Flow Metab. 29 (2009) 820–829.
[29] O. Ullrich, A. Diestel, I.Y. Eyupoglu, R. Nitsch, Regulation of microglial expression of integrins by poly(ADP-ribose) polymerase-1, Nat. Cell Biol. 3 (2001) 1035–1042.
[30] C.C. Alano, T.M. Kauppinen, A.V. Valls, R.A. Swanson, Minocycline inhibits poly(ADP-ribose) polymerase-1 at nanomolar concentrations, Proc. Natl. Acad. Sci. U. S. A. 103 (2006) 9685–9690.
[31] I. Ginis, R. Jaiswal, D. Klimanis, J. Liu, J. Greenspon, J.M. Hallenbeck, TNF-alpha-induced tolerance to ischemic injury involves differential control of NF-kappaB transactivation: the role of NF-kappaB association with p300 adaptor, J. Cereb. Blood Flow Metab. 22 (2002) 142–152.
[32] A. Chiarugi, Poly(ADP-ribose) polymerase: killer or conspirator? The 'suicide hypothesis' revisited, Trends Pharmacol. Sci. 23 (2002) 122–129.
[33] A. Chiarugi, M.A. Moskowitz, Poly(ADP-ribose) polymerase-1 activity promotes NF-kappaB-driven transcription and microglial activation: implication for neurodegenerative disorders, J. Neurochem. 85 (2003) 306–317.
[34] P.O. Hassa, M.O. Hottiger, A role of poly (ADP-ribose) polymerase in NF-kappaB transcriptional activation, Biol. Chem. 380 (1999) 953–959.
[35] Y. Lee, P. Castri, J. Bembry, D. Maric, S. Auh, J.M. Hallenbeck, SUMOylation participates in induction of ischemic tolerance, J. Neurochem. 109 (2009) 257–267.
[36] M. Urabe, C. Ding, R.M. Kotin, Insect cells as a factory to produce adeno-associated virus type 2 vectors, Hum. Gene Ther. 13 (2002) 1935–1943.
[37] J.A. Hillion, K. Takahashi, D. Maric, C. Ruetzler, J.L. Barker, J.M. Hallenbeck, Development of an ischemic tolerance model in a PC12 cell line, J. Cereb. Blood Flow Metab. 25 (2005) 154–162.
[38] Y.J. Lee, S. Miyake, H. Wakita, D.C. McMullen, Y. Azuma, S. Auh, J.M. Hallenbeck, Protein SUMOylation is massively increased in hibernation torpor and is critical for the cytoprotection provided by ischemic preconditioning and hypothermia in SHSY5Y cells, J. Cereb. Blood Flow Metab. 27 (2007) 950–962.
[39] I. Ginis, J.M. Hallenbeck, J. Liu, M. Spatz, R. Jaiswal, E. Shohami, Tumor necrosis factor and reactive oxygen species cooperative cytotoxicity is mediated via inhibition of NF-kappaB, Mol. Med. 6 (2000) 1028–1041.
[40] A. Pellacani, M.T. Chin, P. Wiesel, M. Ibanez, A. Patel, S.F. Yet, C.M. Hsieh, J.D. Paulauskis, R. Reeves, M.E. Lee, M.A. Perrella, Induction of high mobility group-I(Y) protein by endotoxin and interleukin-1beta in vascular smooth muscle cells. Role in activation of inducible nitric oxide synthase, J. Biol. Chem. 274 (1999) 1525–1532.
[41] G. Tellman, LightCycler480 real-time PCR system: innovative solutions for relative quantification, Biochemica 4 (2006) 16–17.
[42] Y. Zhang, T.S. Park, J.M. Gidday, Hypoxic preconditioning protects human brain endothelium from ischemic apoptosis by Akt-dependent survivin activation, Am. J. Physiol. 292 (2007) H2573–H2581.
[43] E. Gerace, T. Scartabelli, L. Formentini, E. Landucci, F. Moroni, A. Chiarugi, D.E. Pellegrini-Giampietro, Mild activation of poly(ADP-ribose) polymerase (PARP) is neuroprotective in rat hippocampal slice models of ischemic tolerance, Eur. J. Neurosci. 36 1993-2005.
[44] M. Isabelle, X. Moreel, J.P. Gagne, M. Rouleau, C. Ethier, P. Gagne, M.J. Hendzel, G.G. Poirier, Investigation of PARP-1, PARP-2, and PARG interactomes by affinity-purification mass spectrometry, Proteome Sci. 8 22.
[45] S. Erener, V. Petrilli, I. Kassner, R. Minotti, R. Castillo, R. Santoro, P.O. Hassa, J. Tschopp, M.O. Hottiger, Inflammasome-activated caspase 7 cleaves PARP1 to enhance the expression of a subset of NF-kappaB target genes, Mol. Cell 46 200-211.
[46] M.E. Smulson, D. Pang, M. Jung, A. Dimtchev, S. Chasovskikh, A. Spoonde, C. Simbulan-Rosenthal, D. Rosenthal, A. Yakovlev, A. Dritschilo, Irreversible binding of poly(ADP)ribose polymerase cleavage product to DNA ends revealed by atomic force microscopy: possible role in apoptosis, Cancer Res. 58 (1998) 3495–3498.
[47] T.M. Yung, M.S. Satoh, Functional competition between poly(ADP-ribose) polymerase and its 24-kDa apoptotic fragment in DNA repair and transcription, J. Biol. Chem. 276 (2001) 11279–11286.

[48] V. Schreiber, D. Hunting, C. Trucco, B. Gowans, D. Grunwald, G. De Murcia, J.M. De Murcia, A dominant-negative mutant of human poly(ADP-ribose) polymerase affects cell recovery, apoptosis, and sister chromatid exchange following DNA damage, Proc. Natl. Acad. Sci. U. S. A. 92 (1995) 4753–4757.
[49] Y. Li, C. Li, L. Sun, G. Chu, J. Li, F. Chen, G. Li, Y. Zhao, Role of p300 in regulating neuronal nitric oxide synthase gene expression through nuclear factor-kappaB-mediated way in neuronal cells, Neuroscience.
[50] J.X. Song, P.C. Shaw, C.W. Sze, Y. Tong, X.S. Yao, T.B. Ng, Y.B. Zhang, Chrysotoxine, a novel bibenzyl compound, inhibits 6-hydroxydopamine induced apoptosis in SH-SY5Y cells via mitochondria protection and NF-kappaB modulation, Neurochem. Int. 57 676-689.
[51] I. Sarnico, A. Lanzillotta, M. Benarese, M. Alghisi, C. Baiguera, L. Battistin, P. Spano, M. Pizzi, NF-kappaB dimers in the regulation of neuronal survival, Int. Rev. Neurobiol. 85 (2009) 351–362.
[52] A. Kunz, T. Abe, K. Hochrainer, M. Shimamura, J. Anrather, G. Racchumi, P. Zhou, C. Iadecola, Nuclear factor-kappaB activation and postischemic inflammation are suppressed in CD36-null mice after middle cerebral artery occlusion, J. Neurosci. 28 (2008) 1649–1658.
[53] O.A. Harari, J.K. Liao, NF-kappaB and innate immunity in ischemic stroke, Ann. N. Y. Acad. Sci. 1207 32-40.
[54] D.C. Bedford, L.H. Kasper, T. Fukuyama, P.K. Brindle, Target gene context influences the transcriptional requirement for the KAT3 family of CBP and p300 histone acetyltransferases, Epigenetics 5 9-15.
[55] P. Tieri, A. Termanini, E. Bellavista, S. Salvioli, M. Capri, C. Franceschi, Charting the NF-kappaB pathway interactome map, PloS One 7 e32678.
[56] P.O. Hassa, M.O. Hottiger, The functional role of poly(ADP-ribose)polymerase 1 as novel coactivator of NF-kappaB in inflammatory disorders, Cell. Mol. Life Sci. 59 (2002) 1534–1553.
[57] P.O. Hassa, M. Covic, S. Hasan, R. Imhof, M.O. Hottiger, The enzymatic and DNA binding activity of PARP-1 are not required for NF-kappa B coactivator function, J. Biol. Chem. 276 (2001) 45588–45597.